Heliyon 10 (2024) e27350

Contents lists available at ScienceDirect

Heliyon

journal homepage: www.cell.com/heliyon

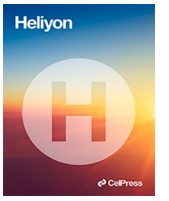

Research article

Activation of the BMP2-SMAD1-CGRP pathway in dorsal root ganglia contributes to bone cancer pain in a rat model

Wei Wang [a,1], Zhihao Gong [a,1], Kai Wang [b], Mi Tian [c], Yuxin Zhang [a], Xin Li [d], Xingji You [d,**], Jingxiang Wu [a,*]

[a] Department of Anesthesiology, Shanghai Chest Hospital, Shanghai Jiao Tong University, School of Medicine, Shanghai 200030, China
[b] Central Laboratory, Shanghai Chest Hospital, Shanghai Jiao Tong University, School of Medicine, Shanghai 200030, China
[c] Department of Intensive Care Medicine, HuaShan Hospital, Fudan University, Shanghai 200040, China
[d] School of Medicine, Shanghai University, Shanghai 200444, China

ARTICLE INFO

Keywords:
BMP2
CGRP
Bone cancer pain
Dorsal root ganglia
Peripheral sensitization

ABSTRACT

Peripheral nerve remodeling and sensitization are involved in cancer-related bone pain. As a member of the transforming growth factor-β class, bone morphogenetic protein 2 (BMP2) is recognized to have a role in the development of the neurological and skeletal systems. Our previous work showed that BMP2 is critical for bone cancer pain (BCP) sensitization. However, the mechanism remains unknown. In the current study, we demonstrated a substantial increase in BMP2 expression in the dorsal root ganglia (DRG) in a rat model of BCP. Knockdown of BMP2 expression ameliorated BCP in rats. Furthermore, the DRG neurons of rats with BCP expressed higher levels of calcitonin gene-related peptide (CGRP), and BCP was successfully suppressed by intrathecal injection of a CGRP receptor blocker ($CGRP_{8-37}$). Downregulation of BMP2 expression reduced the expression of CGRP in the DRG of rats with BCP and relieved pain behavior. Moreover, we revealed that upregulation of CGRP expression in the DRG may be induced by activation of the BMPR/Smad1 signaling pathway. These findings suggest that BMP2 contributes to BCP by upregulating CGRP in DRG neurons via activating BMPR/Smad1 signaling pathway and that therapeutic targeting of the BMP2-Smad1-CGRP pathway may ameliorate BCP in the context of advanced cancer.

1. Introduction

As the second greatest cause of death globally, malignant tumors are expected to account for 13.2 million cancer-related deaths and 22.2 million new cancer cases by 2030 [1]. One of the most frequent side effects of cancer is metastatic bone cancer – it occurs in 65–80% of patients suffering from lung, breast and prostate cancers – and it usually renders the cancer incurable. Bone metastasis usually causes severe bone pain, while the mechanism of this phenomenon remains unclear [2]. Bone cancer pain (BCP) is one of the most intractable forms of pain, as over 50% of individuals with metastatic cancer do not fully recover from their pain [3–5].

Bone morphogenetic proteins (BMPs) are the biggest subclass of the transforming growth factor-β family of ligands, and they are

* Corresponding author.
** Corresponding author.
E-mail addresses: yoyo1976@shu.edu.cn (X. You), wjx1132@163.com (J. Wu).
[1] These authors contributed equally to this work.

https://doi.org/10.1016/j.heliyon.2024.e27350
Received 22 April 2022; Received in revised form 25 February 2024; Accepted 28 February 2024
Available online 4 March 2024

potentially involved in the progression of BCP [6]. In addition to bone development, these factors participate in a myriad of biological processes including gastrulation, embryonic patterning, organogenesis [7], angiogenesis, vascular integrity [8], iron homeostasis [9], inflammation [10,11], and nervous system development and function [6,12]. Bone morphogenetic protein 2 (BMP2) is the only osteoinductive growth factor authorized by the US Food and Drug Administration for bone regeneration and repair [13,14]. In addition to its beneficial effects, BMP2 can induce inflammation and pain [15–18], in part by triggering the production of the tumor necrosis factor (TNF)-α and inflammatory cytokines interleukin (IL)-1β, IL-6, IL-17 and IL-18 [19]. BMP2 can induce neuroinflammation in peripheral nerves and the spinal cord in spinal cord injury patients [20,21], infiltrate the dorsal root ganglia (DRG) and alter its function [22], and upregulate the release of the neuroinflammatory molecule calcitonin gene-related peptide (CGRP) in peripheral sensory neurons in vitro [23].

CGRP is a peptide released from sensory nerves, essential for the perception of pain [24]. Clinical trials investigating CGRP receptor antagonist (erenumab) and monoclonal antibodies (eptinezumab, fremanezumab and galcanezumab) have consistently demonstrated statistically significant efficacy for either the acute or preventative therapy of migraine [25,26]. Much like the trigeminal ganglion, the DRG is one of the primary locations of CGRP synthesis, which indicating that CGRP is broadly dispersed in distinct parts of the central and peripheral nervous systems [24]. According to earlier studies, BMP2 concentration-dependently increases the expression of CGRP in embryonic DRG cells [27]. Previously, we showed that BMP2 is upregulated in DRG neurons in a rat model of BCP, and that an BMP2-targeting siRNA ameliorates pain in vivo [28]. However, the relationship between BMP2 and CGRP has not been reported for BCP. These findings led us to explore in detail the role of BMP2 in peripheral sensitization in BCP. In particular, we wanted to examine whether CGRP may also be involved, given its well-documented role in maintaining chronic pain [29,30].

In order to ascertain if BMP2 and CGRP are increased in the DRG and how these factors contribute to BCP, we employed a rat model of metastatic tibial cancer pain in this study. We discovered that in this model, Walker 256 mammary gland carcinoma cells implantation into the rat tibia upregulates BMP2 and activates the BMPR/Smad1 signaling pathway in the DRG, which in turn causes the overexpression of CGRP. Our findings indicated that the BMP2-Smad1-CGRP signaling pathway may be a possible target for BCP therapy.

2. Materials and methods

All experiments followed protocols approved by the Ethics Committee of Shanghai Chest Hospital [No. KS (Y)20186] and the guidelines for investigations of experimental pain in animals published by the International Association for the Study of Pain [31].

2.1. Experimental design

Walker 256 mammary gland carcinoma cells were implanted into the tibia bone cavity in rats to induce BCP as described [32]. 6–8 weeks old of female Sprague-Dawley rats (Shanghai JieSiJie Laboratory Animals Co., Ltd., Shanghai, China) were injected with either Walker 256 cells (2×10^5 cells in 10 μL) or control saline into the lower third of the right tibia's intramedullary canal using a 23-gauge needle under pentobarbital anesthesia. At the end of the experiment, DRG samples and ipsilateral tibial bones were harvested for analysis.

In the first set of experiments, rats were divided into groups of 14–15 randomly that received an intrathecal administration of 2 μg BMP2-siRNA or scrambled control RNA in 10 μL of in vivo-jetPEI™ (201-10G, Polyplus-transfection, Illkirch, France) or in vivo-jet-PEI™ only on days 10, 12, 14, and 16. The animals were subjected to the von Frey mechanical pain test (see below) immediately before the start of treatment, on the first day of treatment, and then daily during the treatment period. At the end of the experiments on day 17, DRG samples and ipsilateral tibial bones were harvested for analysis.

In the second set of experiments, random groups of 8–10 rats received an intrathecal injection of the BMP receptor (BMPR) antagonist LDN193189 (MedChemExpress, Monmouth Junction, NJ, USA) at a concentration of 4 mg/mL dissolved in 10 μL normal saline (NS) or NS only on days 10, 12, 14, and 16. Behavioral tests were carried out immediately before the start of treatment, on the first day of treatment, and then daily during the treatment period until the end of the experiment on day 17.

In the third set of experiments, random groups of 8–10 rats received an intrathecal injection of CGRP receptor blocker $CGRP_{8\text{-}37}$ (MedChemExpress, Monmouth Junction, NJ, USA) at a concentration of 50 nM dissolved in 10 μL NS, or NS only on day 17 [29]. Behavioral tests were carried out at 10 min, 20 min, 30 min, 1 h, 2 h and 4 h post-injection.

2.2. Behavioral tests

Mechanical pain was assessed using a standard von Frey test. In brief, rats were housed in a cage with a metal-mesh floor, and a von Frey monofilament was applied perpendicularly to the plantar surface of the hindpaw on the ipsilateral side of the lesions; the intensity of application was raised (0.6, 1.0, 1.4, 2, 4, 6, 8, 10, and 15 g) until the paw was removed. Every stimulation lasted roughly 3 s. 5 min apart, each monofilament was applied five times. Paw flinching or a rapid retreat was regarded as a favorable reaction. Based on 5 applications, the paw withdrawal mechanical frequency (PWMF) in reaction to every monofilament was computed. The force at which PWMF $\geq$60% was determined to be the paw withdrawal mechanical threshold (PWMT). The PWMT was recorded at 15 g if PWMF was less than 60% for every filaments [33]. We repeated the test 3 times and calculated the average PWMT for analysis.

Limb use scores was used to assess movement-evoked pain [33,34]. The rats were allowed to move around unrestrictedly on a 50 cm × 50 cm smooth plastic table. A scale of 4 to 0 was used to rate limb usage during spontaneous ambulation (4, normal; 3, slight limp; 2, obvious limp; 1, partial use of limbs; 0, no use of limbs). Three repeated estimations were conducted and the average was

calculated for analysis.

2.3. Micro-computerized tomography (Micro-CT)

As previously mentioned, the ipsilateral tibia of sham and BCP rats were taken and scanned using a 55-kVp source of VivaCT 80 scanner (Scanco, Southeastern, PA) [3]. The proximal 1/3 of the tibia was observed as the area of interest. Images were acquired for 3D reconstruction using Scanco Medical software.

2.4. Histomorphological analysis of bone

The affected tibia of rats with BCP was fixed in 4% paraformaldehyde for 48 h, then decalcified in 10% EDTA for a period of 3–4 weeks, thereafter 6-μm slices were acquired on a rotating microtome. Following paraffin embedding, the slices were deparaffinized by xylene, rehydrated, and stained with hematoxylin–eosin dyeing reagent (H&E; Sigma, St Louis, MO, USA).

2.5. Immunofluorescence

Rats were given an overdose of intraperitoneal pentobarbital and transcardially perfused with 100 mL of 4 °C phosphate-buffered saline (PBS) and 200 mL of 4% paraformaldehyde. The L3-L5 DRGs were fixed in 4% paraformaldehyde overnight and dehydrated in 30% sucrose. DRG samples were embedded in SAKURA Tissue-Tek® O.C.T. Compound (Sakura Finetek, Torrance, CA, USA), cut into 5-μm slices using a CM1850-1-1 cryostat (Leica, Wetzlar, Germany) and then mounted on slides. To remove remanent OCT, each DRG sample was thoroughly washed in PBS. The samples were blocked for 1 h in PBS containing 0.3% Triton-X 100 and 5% normal donkey serum, then incubated overnight with rabbit polyclonal antibody (pAb) against BMP2 (1:500, ab14933; Abcam), mouse monoclonal antibody (mAb) against NeuN (1:1000, ab104224, Abcam), mouse mAb against GFAP (1:500, GB12096, Servicebio, Wuhan, China), rabbit pAb against NeuN (1:500, GB11138, Servicebio, Wuhan, China), mouse mAb against CGRP (1:500, sc-57053; Santa Cruz Biotechnology, Santa Cruz, CA, USA), rabbit mAb against phospho-Smad1 (Ser463/465) (1:800, #13820; Cell Signaling Technology), or rabbit pAb against c-Fos (1:500, GB11069, Servicebio, Wuhan, China). The samples were washed in PBS the following day and treated for 1 h in PBS containing the relevant secondary antibody (1:500) from Cell Signaling Technology (catalog nos. 8889 or 4408) or Jackson ImmunoResearch (catalog nos. 711-545-152 or 715-585-150). The samples were then coverslipped with Antifade Mounting Medium containing DAPI (Beyotime, Nanjing, China) after being washed in PBS. A TCS SP8 confocal microscope (Leica Microsystems, Mannheim, Germany) was used for imaging and analysis. A blinded quantitative histomorphometric analysis was carried out using Image Lab software (ImageJ, Version 2.0.0-rc-69/1.52p, https://imagej.net/). We chose one optimal section out of 5 sections per rat and counted the number and calculated the ratio of positively stained cells in the whole DRG area in each group.

2.6. Real-time quantitative polymerase chain reaction (RT-qPCR)

Using the RNA-easy Isolation Reagent (Vazyme Biotech, Nanjing, China), total RNA was isolated from L3-L5 DRG. A complementary DNA (cDNA) Synthesis Kit (DBI® Bioscience, Ludwigshafen, Germany) was then used to generate cDNA. Utilizing a StepOnePlus™ Real-Time PCR System (Applied Biosystems®, Thermo Fisher Scientific, Waltham, MA, USA), RT-qPCR was performed using a SYBR Green assay (DBI® Bioscience). The following primers were used in the study: BMP2 sense, 5'-AAGCCAGGTGTCTCCAAG-3'; BMP2 antisense, 5'-AAGTCCACATACAAAGGGTG-3'; Calca (which encodes CGRP) sense, 5'-GGAGCAGGAGGAGGAACAGGAG-3'; Calca antisense, 5'-CTAAGCAACCAGGTGACCAG-3'; GAPDH sense, 5'-GGTGGACCTCATGGCCTACA-3'; GAPDH antisense, 5'-CTCTCTTGCTCTCAGTATCCTTGCT-3'. Relative gene expression was normalized to the expression of GAPDH mRNA and determined using the $2^{-\Delta\Delta Ct}$ method.

2.7. Western blotting

The L3-L5 DRGs underwent 2 centrifugations at 13,800 g for 20 min at 4 °C after being homogenized. A bicinchoninic acid assay kit (Solarbio, Beijing, China) was used to assess the protein concentration in the supernatant. Using 10% SDS-polyacrylamide gel electrophoresis, samples (50 μg) were fractionated and then transferred onto nitrocellulose membranes. They were then blocked for 1–2 h at room temperature using 5% nonfat milk in Tris-buffered saline (TBS; 50 mM Tris-HCl and 150 mM NaCl, pH 7.5). Finally, they were incubated for an additional night at 4 °C in TBS containing Triton X-100 (TBST) in 1% nonfat milk with primary antibodies against the following: BMP2 (1:500, ab14933; Abcam, Cambridge, UK), BMPR1B (1:1000, ab175385; Abcam), BMPR2 (1:500, AF5383; Affinity Biosciences, OH, USA), Smad1 (1:500, ab131550, Abcam), phospho-Smad1 (S465) (1:500, ab97689, Abcam), and GAPDH (1:2000, BL006B; Biosharp Life Sciences, Hefei, Anhui, China). Following three washes with TBST, the membranes were incubated for 1–2 h at room temperature with a secondary antibody (1:2000, #7074; Cell Signaling Technology, MA, USA) couple to horseradish peroxidase in TBST containing 1% milk. The membranes were analyzed with a computerized image analysis system (ChemiDoc XRS1, Bio-Rad, Hercules, CA). Using Image Lab software (ImageJ, Version 2.0.0-rc-69/1.52p, https://imagej.net/), the intensity of the protein bands was measured. Target protein expression was normalized against that of GAPDH.

2.8. Knockdown of BMP2 in the BCP model

Three siRNAs were designed to knock down BMP2 (GenePharma, Shanghai, China). Successful intrathecal injection of siRNAs interfering the DRG were confirmed by immunofluorescent microscopic imaging (Figs. S1A–C). Pilot experiments showed that the sequences BMP2-404-siRNA sense (5'-GAAGCCAUCGAGGAACUUUTT-3') and BMP2-404-siRNA antisense (5'-AAA-GUUCCUCGAUGGCUUCTT-3') achieved the greatest knockdown when injected intrathecally into naïve rats (Fig. S1D). They were therefore used in all subsequent experiments.

2.9. Statistical analysis

All results are expressed as mean ± standard deviation. The data were analyzed using GraphPad Prism 8.0 for Windows (GraphPad, San Diego, CA, USA). All behavioral tests and other experiments were performed in a blinded manner. Data from behavioral tests were analyzed using two-way repeated-measures analysis of variance (ANOVA), followed by Tukey's post hoc test. For other data,

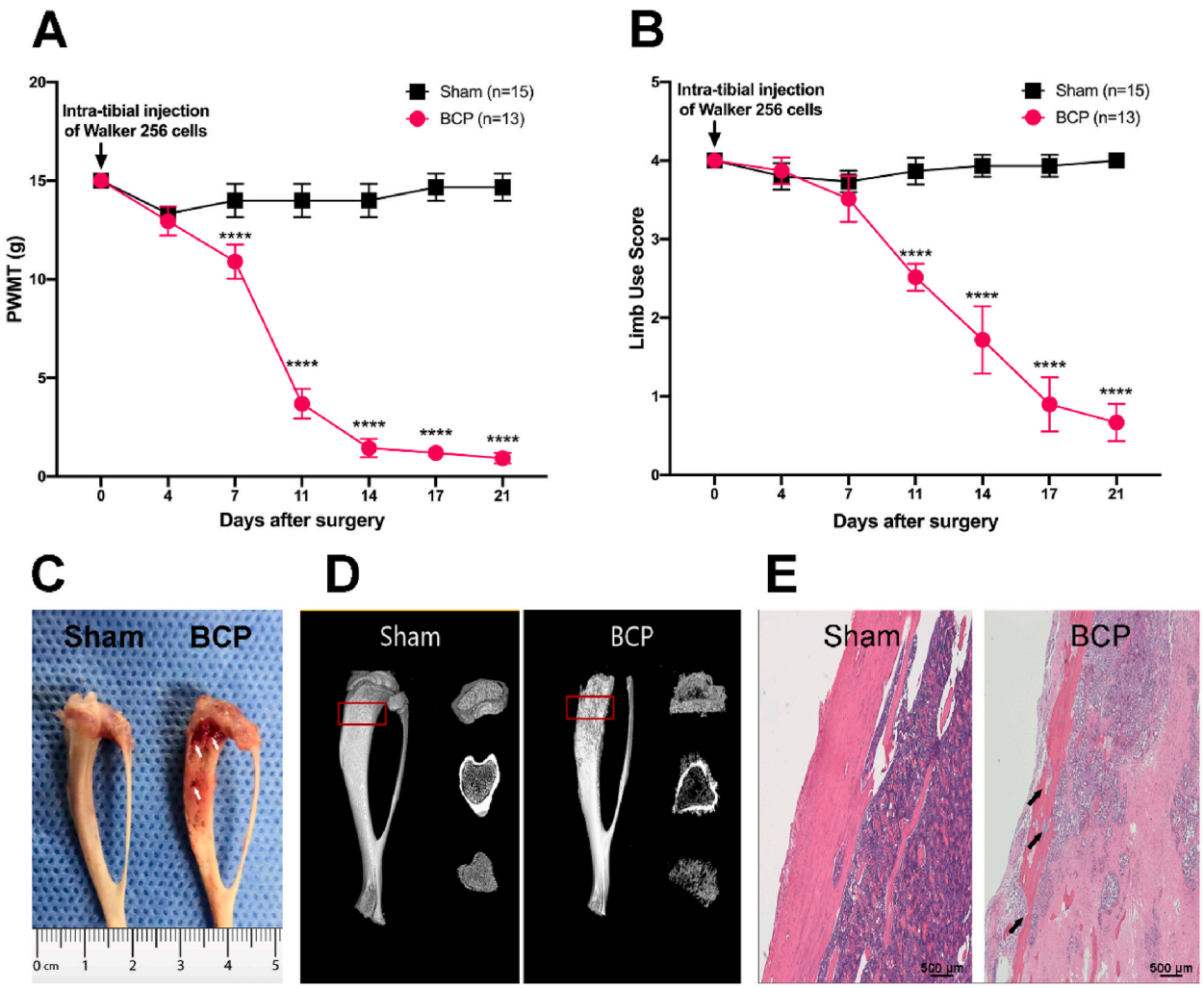

Fig. 1. Injection of Walker 256 mammary gland carcinoma cells into the tibia promotes pain behaviors and bone remodeling in rats. (A) Intratibial inoculation of Walker 256 mammary gland carcinoma cells (BCP group) induced significant mechanical hyperalgesia in the hindpaw ipsilateral to the tumor-bearing hindpaw. PWMT, paw withdrawal mechanical threshold (****$p < 0.0001$); two-way ANOVA with the Geisser-Greenhouse correction and Tukey's multiple comparisons test. (B) Limb use score in sham and BCP group rats. See methods for description of limb scoring (****$p < 0.0001$); two-way ANOVA with the Geisser-Greenhouse correction and Tukey's multiple comparisons test. (C) Representative photograph of a rat tibia from the BCP group (n = 13) on day 21 showing obvious tumor growth and bone mass loss compared to a representative rat tibia from the sham group (n = 15). (D) Representative micro-CT images showing the bone microstructure of the tibia of a sham and BCP rat 21 days after tumor inoculation. Reduction in the medullary bone and increase in cortical bone lesions are visible in rats with BCP. n = 6 per group. (E) Representative histological images after hematoxylin and eosin staining showing medullary bone loss and tibial bone damage in rats with BCP on day 21. n = 6 per group. Scale bar: 500 μm.

comparisons between two groups were analyzed using two-tailed unpaired Student's t-tests, and comparisons among more than three groups were analyzed using one-way ANOVA followed by Tukey's post hoc test. Differences for which the p-value was less than 0.05 were considered statistically significant.

3. Results

3.1. BMP2 and BMPRs are critical for BCP progression

Starting on day 7, the PWMT diverged between rats that received an intratibial administration of Walker 256 cells (BCP group) and control rats that received administration of normal saline (sham surgery) (Fig. 1A). On day 14, rats in the BCP group became highly sensitive to mechanical pain, the PWMT stabilized at < 2 g, and limb use became increasingly limited (Fig. 1A and B). On day 21, in the BCP group, tumor growth and tibia bone mass loss were seen compared to the sham group in photographs (Fig. 1C), micro-CT images (Fig. 1D), and histological analysis (Fig. 1E).

We next assessed BMP2 expression in both rat groups. Double immunofluorescence staining revealed a significantly higher density of BMP2-positive neurons (Fig. 2A and B) and BMP2 expression at both the mRNA (Fig. 2C) and protein (Fig. 2D) levels in the L3-L5 DRGs (hereafter simply "DRG") of rats with BCP than sham controls. In the meantime, considering satellite glial cell composes most of the glial cells in the DRG, we stained BMP2 with GFAP in the DRG of rats with BCP and the results showed that they were partially co-localized (Fig. S2).

Furthermore, intrathecal injection of a BMP2-targeting siRNA in rats with BCP ameliorated both the PWMT (Fig. 3A) and mechanical hypersensitivity in the affected hindpaw (Fig. 3B). We verified that the siRNA knocked down BMP2 using RT-qPCR (Fig. 3C) and Western blotting (Fig. 3D). To confirm the effect of bone destruction on behavioral changes, we acquired micro-CT images of the tibias of BCP + NC group and BCP + BMP2-siRNA group postmortem after treatment, and the results showed insignificant difference of destructed bone structure (Fig. S3).

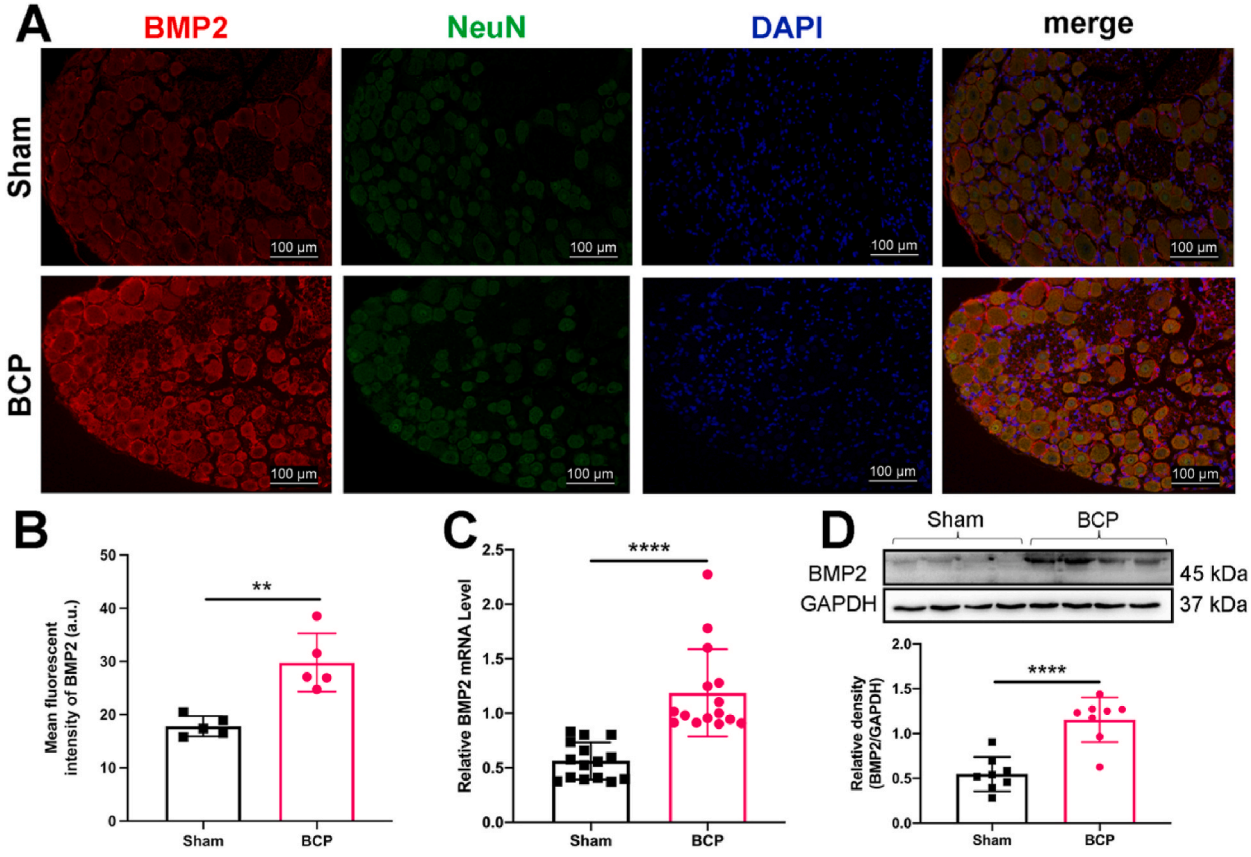

Fig. 2. Expression and cellular localization of BMP2 in the DRG. (A) Immunohistochemistry assessing BMP2 expression in sham and BCP rats on day 21. NeuN was used to stain neurons, and DAPI was used to stain cellular nuclei. Scale bar: 100 μm. (B) Mean fluorescent density of BMP2 in panel (A). n = 5 per group. $t = 4.604$, df = 8. $^{**}p = 0.0017$ (unpaired *t*-test). (C) The mRNA level of BMP2 measured by real-time RT-qPCR and normalized to the level of GAPDH. n = 15 per group. $^{****}p < 0.0001$ (Mann Whitney test). **(D)** Western blot analysis of BMP2 protein levels in L3-L5 DRG on day 21. Top: representative Western blots. Bottom: quantification of BMP2 expression levels. n = 8 per group. $t = 5.451$, df = 14. $^{****}p < 0.0001$ (unpaired *t*-test).

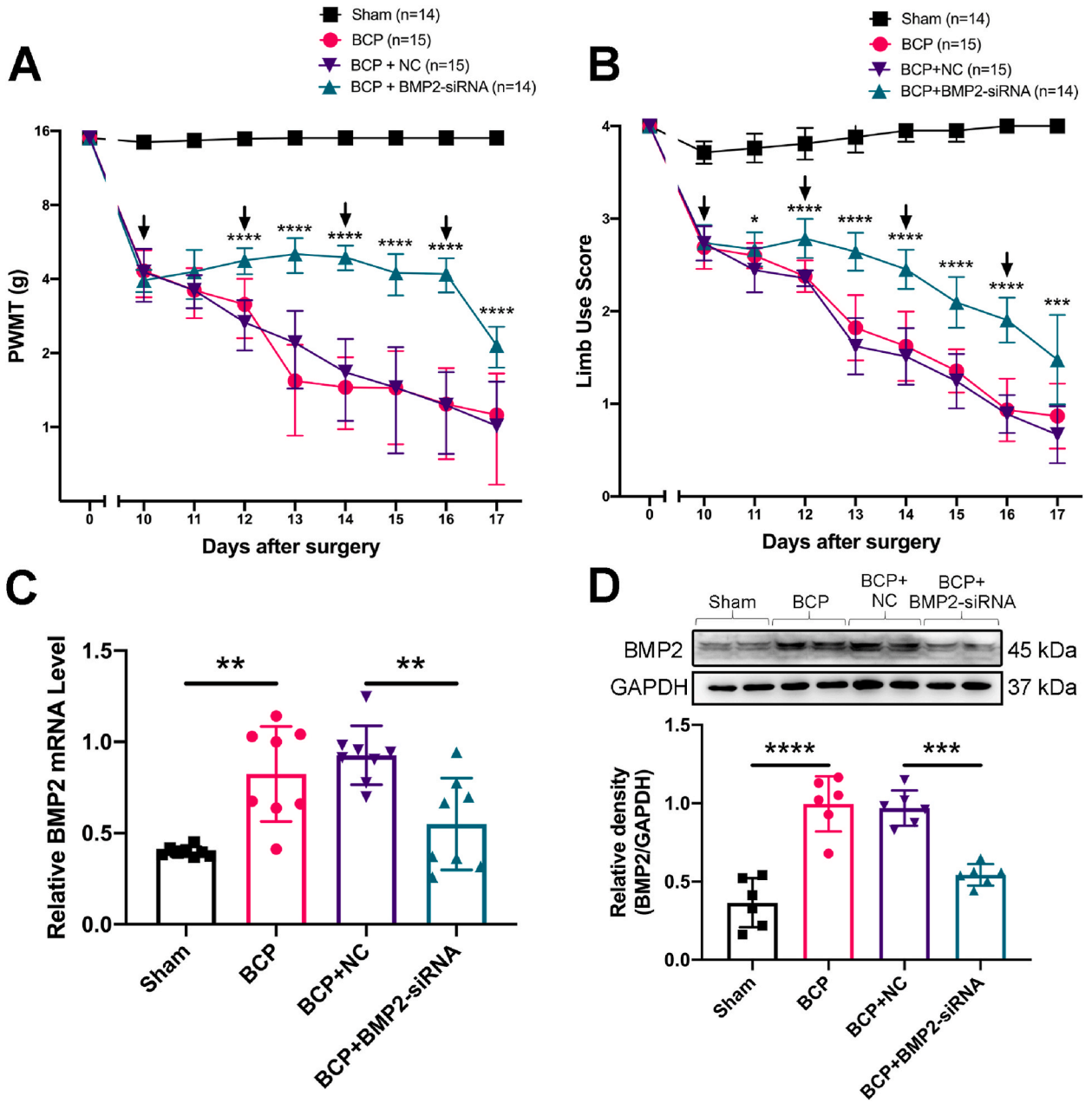

Fig. 3. Knockdown of BMP2 expression ameliorates BCP in rats. (A) Paw withdrawal mechanical threshold (PWMT) in animals subjected to BCP or not (sham), then treated with an siRNA targeting BMP2 or a scrambled negative control siRNA (*$p = 0.0495$, ****$p < 0.0001$ between BCP + BMP2-siRNA group and BCP + NC group); two-way ANOVA with the Geisser-Greenhouse correction and Tukey's multiple comparisons test. (B) Limb use scores (*$p = 0.0446$, ***$p = 0.0001$ for day 10 and 17, ****$p < 0.0001$ between BCP + BMP2-siRNA group and BCP + NC group); two-way ANOVA with the Geisser-Greenhouse correction and Tukey's multiple comparisons test. (C) The mRNA level of BMP2 measured by real-time RT-qPCR and normalized to the mRNA level of GAPDH (n = 8 per group, $F_{(3,28)} = 11.98$, **$p = 0.0011$ and 0.0038 for BCP group vs. sham group and BCP + BMP2-siRNA group vs. BCP + NC group respectively); ordinary one-way ANOVA with Tukey's multiple comparisons test. (D) Western blot analysis of BMP2 levels in L3-L5 DRG ipsilateral to the tumor-bearing bone on day 17 (n = 6 per group, $F_{(3,20)} = 32.54$, ***$p = 0.0001$, ****$p < 0.0001$); ordinary one-way ANOVA with Tukey's multiple comparisons test. Top: representative Western blots. Bottom: quantification of BMP2 expression levels. NC, scrambled negative control siRNA.

We next evaluated the expression of BMPRs. In rats with BCP, BMPR1B (Fig. 4A) and BMPR2 (Fig. 4B) were significantly upregulated in the DRG compared to sham rats. Intrathecal injection of the BMPR antagonist LND193189 into rats with BCP notably increased the PWMT for mechanical stimulation (Fig. 4C) and ameliorated limb use (Fig. 4D).

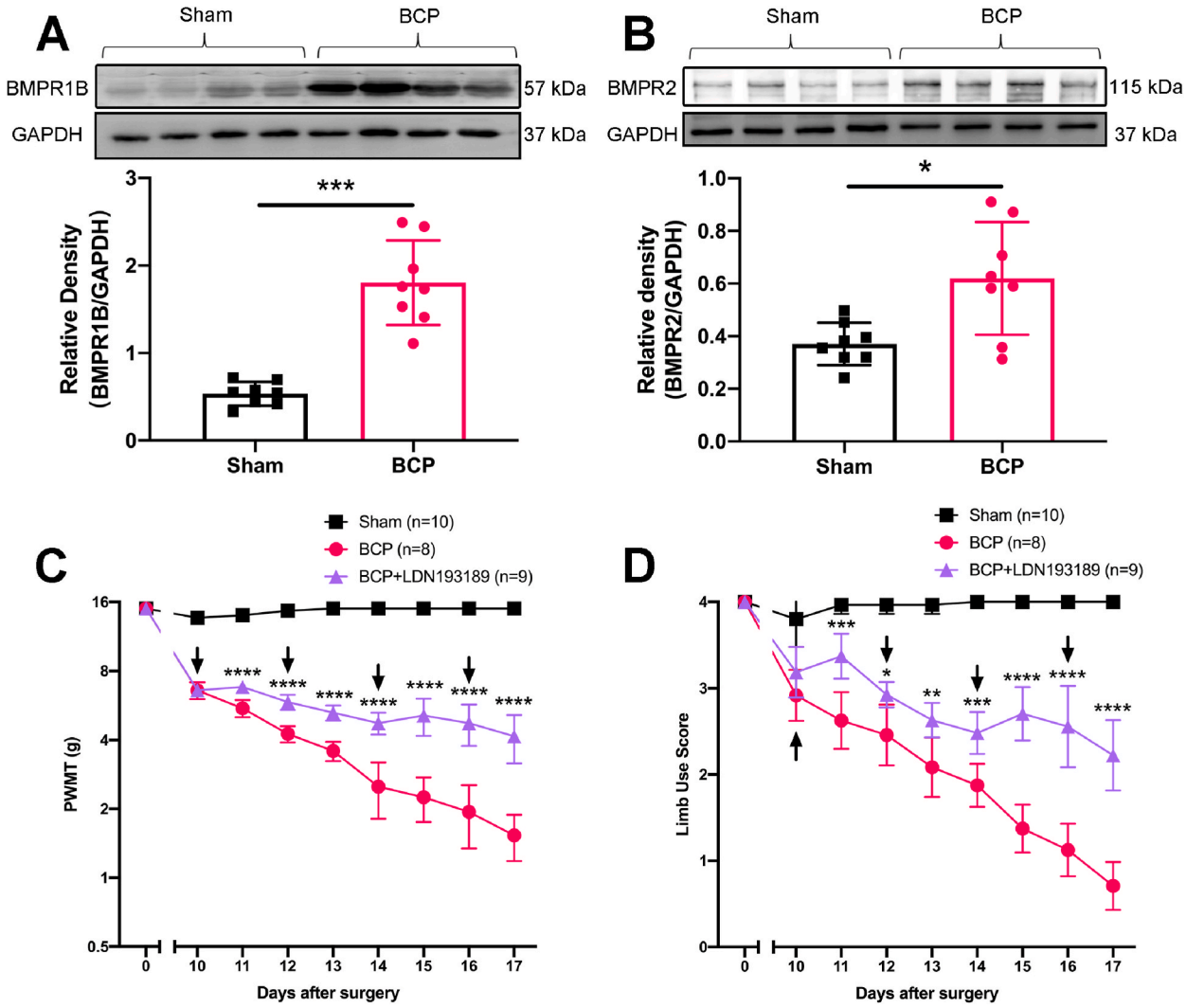

Fig. 4. BMPRs are involved in BCP. (A) Western blot analysis of BMPR1B levels in the L3-L5 DRG ipsilateral to the tumor-bearing bone in rats with BCP versus sham controls on day 21. n = 8 per group. ***$p = 0.0002$ (Mann Whitney test). Top: representative Western blot. Bottom: quantification of BMPR1B expression levels. (B) Western blot analysis of BMPR2 levels in rats with BCP versus sham control rats. n = 8 per group. *$p = 0.0281$ (Mann Whitney test). Top: representative Western blot. Bottom: quantification of BMPR2 expression levels. (C) Paw withdrawal mechanical threshold (PWMT) in BCP animals given LDN193189 or vehicle (****$p < 0.0001$); two-way ANOVA with the Geisser-Greenhouse correction and Tukey's multiple comparisons test. (D) Limb use scores in BCP animals given LDN193189 or vehicle (*$p = 0.0168$, **$p = 0.0062$, ***$p = 0.0005$ and 0.0004 for day 11 and day 14 respectively, ****$p < 0.0001$); two-way ANOVA with the Geisser-Greenhouse correction and Tukey's multiple comparisons test.

3.2. BMP2 stimulates phosphorylation of Smad1

As the canonical downstream target of BMP2, phosphorylation of Smad1 is important for the transduction of biological signals [35, 36]. In the present study, rats with BCP showed much higher levels of phosphorylated Smad1 (pSmad1) in the DRG compared to sham rats. Conversely, BMP2 knockdown significantly decreased pSmad1 levels in the DRG (Fig. 5).

3.3. BMP2 drives BCP via Smad1 phosphorylation-mediated CGRP upregulation

In the present study, double immunofluorescence staining revealed a significantly higher density of CGRP-positive neurons (Fig. 6A and B) and CGRP expression (Fig. 6C and D) in the DRG of rats with BCP than in sham controls. While intrathecal injection of $CGRP_{8\text{-}37}$ significantly ameliorated the PWMT (Fig. 6E) and limb use (Fig. 6F) of rats with BCP.

Furthermore, the double immunofluorescence staining showed co-localization of BMP2 and CGRP in the DRG neurons. (Fig. 7A). The percentage of BMP2-CGRP double-labeled neurons increased significantly in rats with BCP than that of sham rats (Fig. 7B), with a

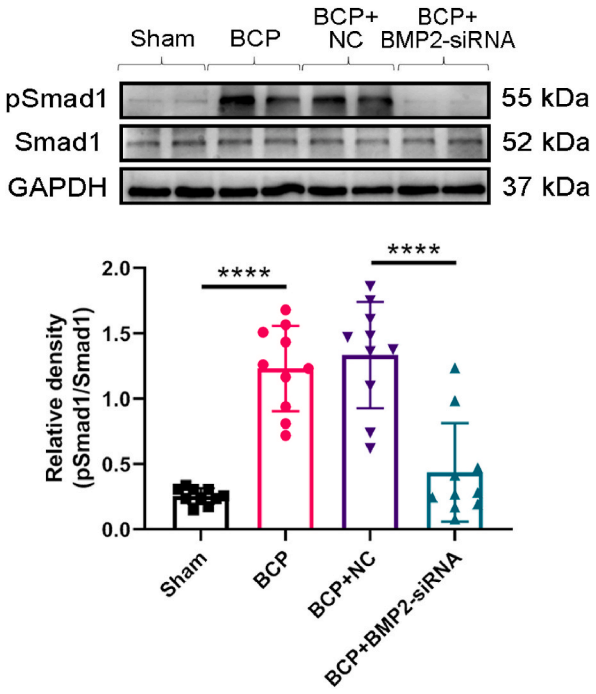

Fig. 5. BMP2 affects Smad1 phosphorylation levels. Western blot analysis of pSmad1 levels in the L3-L5 DRG ipsilateral to the tumor-bearing bone on day 17 after BMP2-siRNA i.t. injection (n = 10 per group, $F_{(3,36)} = 28.68$, $^{****}p < 0.0001$); ordinary one-way ANOVA with Tukey's multiple comparisons test. NC, scrambled negative control siRNA. Top: representative Western blot bands. Bottom: quantification of pSmad1 expression levels.

concurrent increase in cells positive for pSmad1 and CGRP (Fig. 7C and D). BMP2 knockdown decreased the number of DRG cells positive for pSmad1 and CGRP (Fig. 7C and D). Additionally, intrathecal injection of BMP2-siRNA is related to decreased expression level of CGRP in the DRG (Fig. 7E). To confirm the effect of CGRP on the central nervous system, we tested c-Fos expression in the spinal dorsal horn (SDH) among different groups, and the results demonstrated that c-Fos expression was upregulated in BCP group and BCP + Vehicle group compared to Sham group, while intrathecal injection of $CGRP_{8\text{-}37}$ did not decrease the expression of c-Fos in the SDH when compared to the BCP + Vehicle group (Fig. S4).

4. Discussion

Our study provides the evidence that BMP2 contributes to BCP in rats by upregulating the expression of CGRP in sensory neurons in the DRG. To be specific, we observed elevated expression of BMP2 and its receptors, BMPR1B and BMPR2, in the DRG of rats with BCP. Intrathecal injection of BMP2-siRNA obviously decreased BMP2 transcription and relieved BCP. Additionally, the application of BMPR antagonist LDN193189 significantly suppressed bone cancer-induced hyperalgesia, confirming the critical role of BMP2 in BCP progression. BMP2 localized predominantly in sensory neurons and co-localized with CGRP in the DRG, and the BMPR/Smad1 signaling pathway downstream of BMP2 was activated in rats with BCP. We observed upregulation of CGRP in the DRG of rats with BCP and found that administration of a CGRP receptor blocker (CGRP8-37) potently inhibited BCP. Administration of BMP2-siRNA or a specific BMPR inhibitor is associated with downregulation of CGRP in the DRG, and also alleviating BCP (Fig. 8). These findings suggest that BMP2 contributes to BCP by activating the BMPR2/Smad1 signaling pathway in sensory neurons, thereby upregulating CGRP. Our results imply that targeting BMP2 and/or its downstream signaling pathway may ameliorate BCP in advanced cancer.

In our previous study, we discovered that the expression of BMP2 was significantly increased in the DRG of rats with BCP. In the present study, we confirmed the upregulation of BMP2 and found that the knockdown of BMP2 expression in the DRG significantly ameliorated pain manifestations of rats with BCP, indicating that BMP2 is associated with the progression of BCP. As the application of BMP2 in clinical situations increases, side effects of which are often reported. For example, BMP2 used in lumbar fusion is reported to cause bone resorption accompanied by severe nerve injury, leading to the formation of pain [37,38]. Additionally, BMP2, a member of the TGF-β superfamily, is connected to the development of tumor by inducing the epithelial to mesenchymal transition, and further accelerates osteolysis and triggers pain [39]. Also, BMP2 is known to be chemotactic for lymphocytes, monocytes, and macrophages [40]. Recently, postoperative pain in clinical arthrodesis patients treated with BMP2 has been reported, accompanied by a robust inflammatory response of the nerve root [37,41]. This phenomenon is also verified in a rat model of posterolateral arthrodesis [22]. Furthermore, BMP signaling interactions with additional morphogens and signaling pathways are essential for inflammation [12,42]. These studies support that BMP2 can increase local inflammation, leading us to hypothesize that the upregulation of BMP2 in the DRG

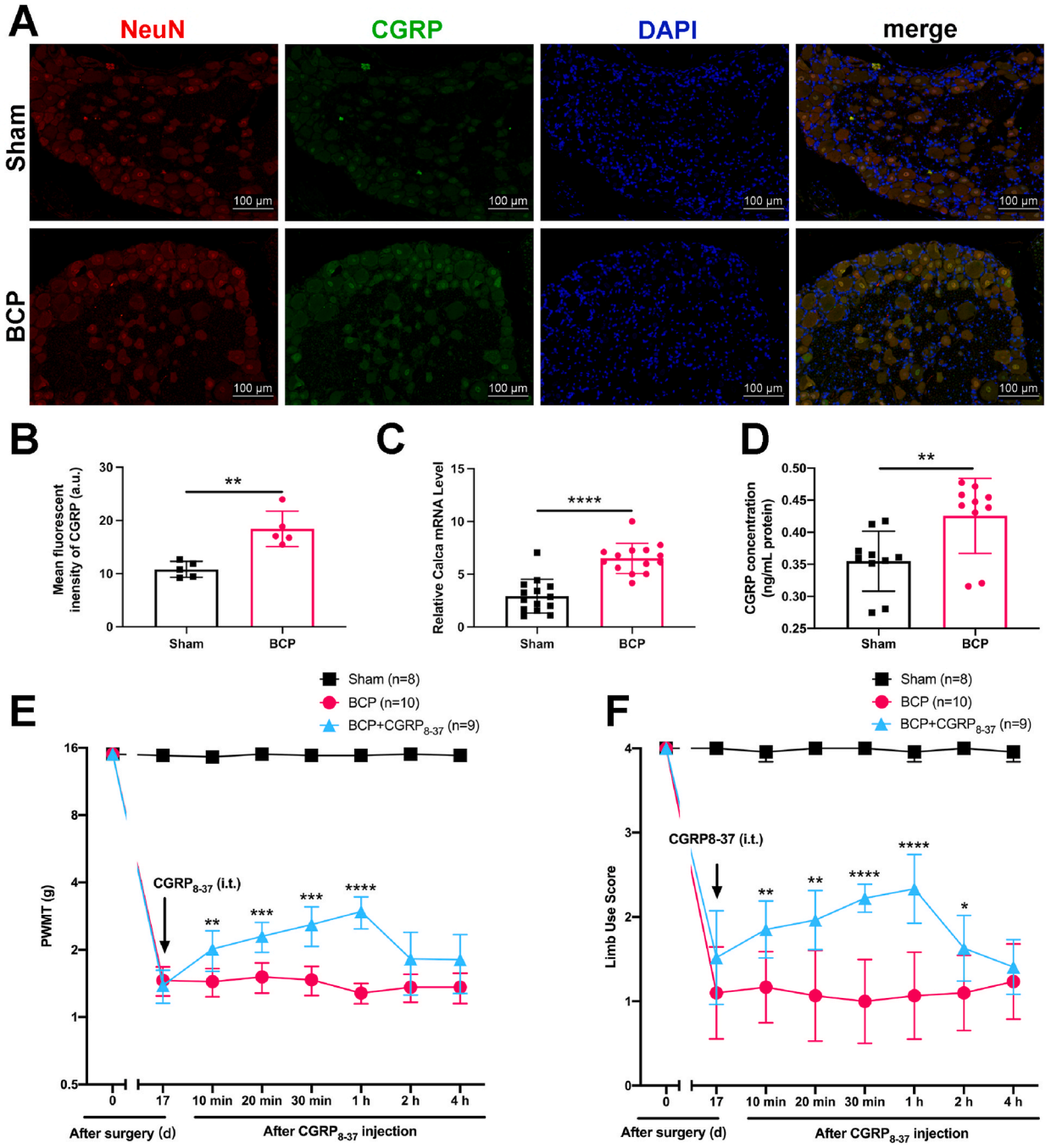

Fig. 6. CGRP participates in the progression of BCP. (A) Immunofluorescence assessing CGRP expression and localization on day 21. Scale bar: 100 μm. (B) Mean fluorescent density of CGRP in panel (A). n = 5 per group. $t = 4.660$, df = 8. $^{**}p = 0.0016$ (unpaired *t*-test). (C) The mRNA level of Calca measured by real-time RT-qPCR and normalized to the mRNA level of GAPDH. n = 14 per group. $t = 6.203$, df = 26. $^{****}p < 0.0001$ (unpaired *t*-test). (D) ELISA assessing the protein level of CGRP in the L3-L5 DRG ipsilateral to the tumor-bearing bone on day 21. n = 10 per group. $t = 2.992$, df = 18. $^{**}p = 0.0078$ (unpaired *t*-test). **(E)** Paw withdrawal mechanical threshold (PWMT) in the BCP animals treated or not with the peptide $CGRP_{8\text{-}37}$ by intrathecal (i.t.) injection ($^{**}p = 0.0075$, $^{***}p = 0.0002$ and 0.0003 for 20 min and 30 min after $CGRP_{8\text{-}37}$ i.t. injection respectively, $^{****}p < 0.0001$); two-way ANOVA with the Geisser-Greenhouse correction and Tukey's multiple comparisons test. (F) Limb use score after $CGRP_{8\text{-}37}$ i.t. injection ($^{*}p = 0.0336$, $^{**}p = 0.0031$ and 0.0015 for 10 min and 20 min after $CGRP_{8\text{-}37}$ i.t. injection respectively, $^{****}p < 0.0001$); two-way ANOVA with the Geisser-Greenhouse correction and Tukey's multiple comparisons test.

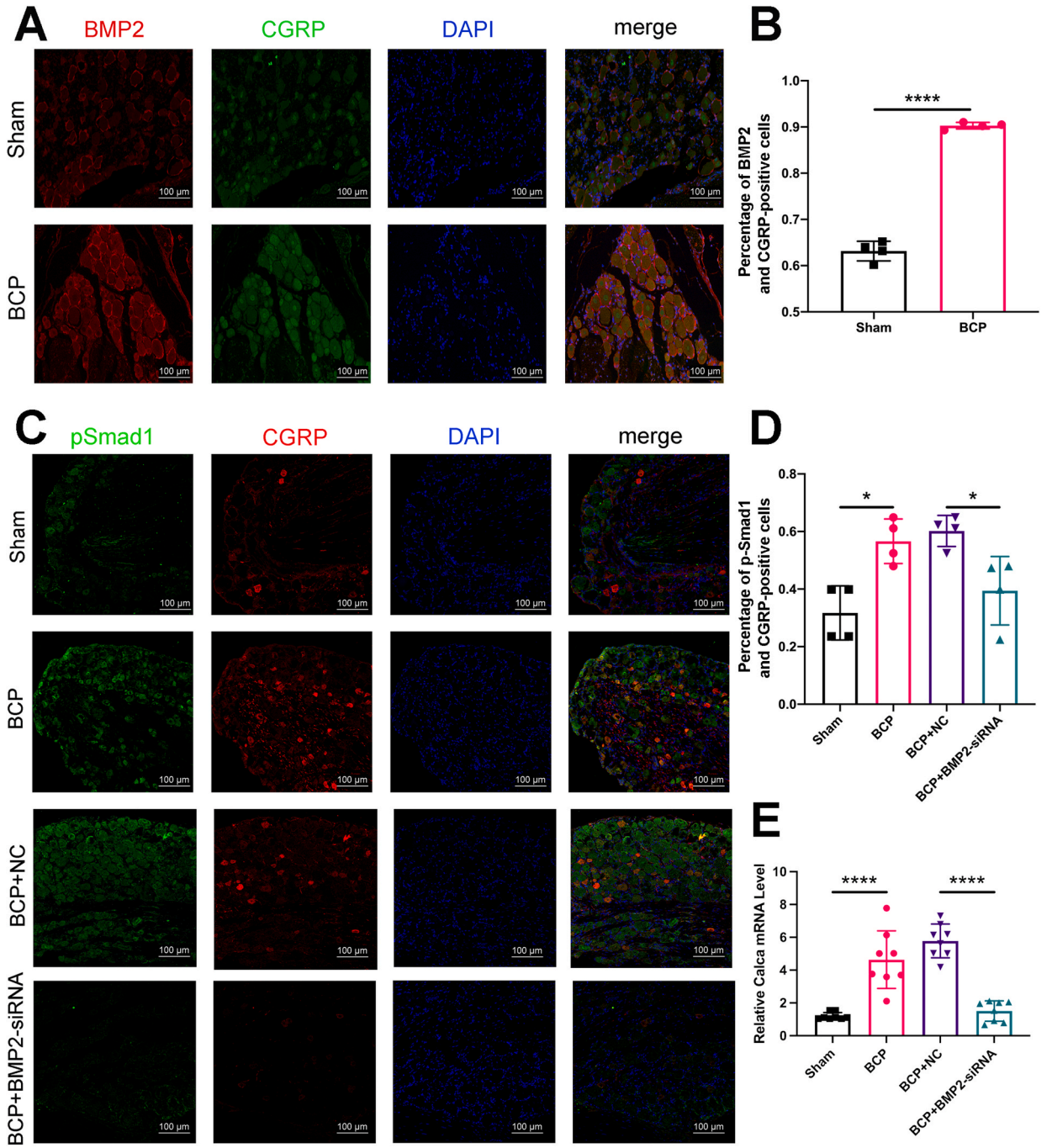

Fig. 7. BMP2 regulates CGRP expression through BMP2/Smad1 signaling in rats with BCP. (A) Double immunofluorescence showing co-localization of BMP2 and CGRP in the DRG of sham and BCP rats on day 21. Scale bar: 100 μm. (B) Percentage of BMP2 and CGRP-positive cells in panel (A). n = 4 per group. $t = 24.15$, df = 6. $^{****}p < 0.0001$ (unpaired t-test). (C) Double immunofluorescence showing co-localization of pSmad1 and CGRP in the DRG of sham and BCP rats after BMP2-siRNA i.t. injection. NC, scrambled negative control siRNA. Scale bar: 100 μm. (D) Percentage of p-Smad1 and CGRP-positive cells in panel (C) ($F_{(3,12)} = 9.307$, $^{*}p = 0.0117$ and 0.0383 for BCP group vs. sham group and BCP + BMP2-siRNA group vs. BCP + NC group respectively); ordinary one-way ANOVA with Tukey's multiple comparisons test. (E) The mRNA level of Calca after i.t. injection of BMP2-siRNA measured by real-time RT-qPCR and normalized to the mRNA level of GAPDH (n = 8 per group. $F_{(3,28)} = 36.40$, $^{****}p < 0.0001$); ordinary one-way ANOVA with Tukey's multiple comparisons test.

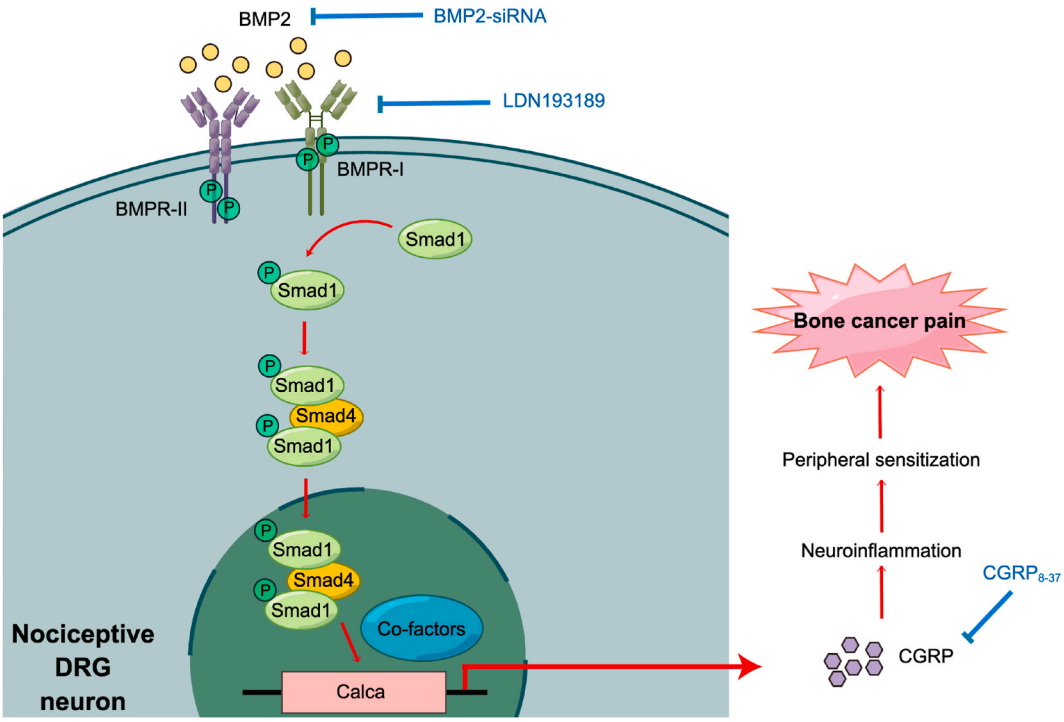

Fig. 8. Schematic summary of the mechanism of the role of BMP2 and the BMPR/Smad1 signaling pathway in the modulation of CGRP expression and progression of BCP. In the nociceptive DRG neurons of rats with BCP, upregulated BMP2 activated downstream BMPR/Smad1 signaling, and increased the release of CGRP, leading to neuroinflammation and contributing to the progression of BCP. This figure was created on Figdraw (www.figdraw.com).

can induce local neuroinflammation and contribute to BCP.

Certain types of pain are mediated by sensory neuropeptides, such as CGRP, which are indicators of nociceptive neurons. As the most widely expressed neuropeptide in mammalian sensory systems, CGRP is a 37-amino acid peptide that is mostly found in C and Aδ sensory fibers [24,43,44]. When peripheral inflammatory events, such as nociceptive behaviors, occurs, endogenous CGRP is crucial in causing plastic neurogenic alterations [24,45,46]. Moreover, CGRP upregulation in DRG neurons is known to be responsible for maintaining chronic pain [29,30]. Therefore, understanding how neuropeptides are regulated following damage is crucial to our comprehension of pain. In this study, we discovered significant upregulation of CGRP in the DRG of rats with BCP, which we linked to the pain phenotype by showing that administration of a peptide antagonist ($CGRP_{8-37}$) attenuated hyperalgesia in the affected hindpaw. Recombinant activin or related BMP2, BMP4, or BMP6 have been shown to concentration-dependently trigger neuropeptide expression in naive embryonic rat sensory neurons, with CGRP expressed by about 60% of these neurons [47]. Likewise, in embryonic DRG cells, BMP2 concentration-dependently increases the expression of CGRP [27]. The current study significantly supports the hypothesis put forth by these earlier studies, which states that overexpressed BMP2 in the DRG raises CGRP expression and causes BCP. In our study, BMP2 co-localized with CGRP in sensory neurons in the DRG, and knockdown of BMP2 expression in the DRG is associated with the suppression of CGRP expression and reduced pain hypersensitivity in rats with bone cancer.

BMP2 must attach to particular receptors to initiate a signaling cascade that triggers different cellular reactions [40]. Thus far, four BMP type I receptors (BMPRIs) and three distinct BMP type II receptors (BMPRIIs) and have been characterized [48]. In this study, BMPR1B and BMPR2 levels in the DRG significantly increased after the progression of BCP, and intrathecal administration of BMPR antagonist LDN193189 significantly relieved BCP, suggesting that the receptor is essential for the progression of BCP. Furthermore, the Smad pathway is activated when BMPR phosphorylate the downstream proteins Smad1/5/8: Smad4 is recruited by phosphorylated Smads, and the resultant complex translocates as a transcription factor into the nucleus [35]. Except for this canonical signaling pathway, non-canonical BMP signaling pathways that are not dependent on Smads have also been discovered, including various branches of the MAPK pathway as well as the PI3K/AKT, JNK/P38, and Rho-GTPase pathways [49–51]. While nociceptive sensitization in Drosophila is proved to be related to BMP signaling via the canonical Smad pathway [36]. Moreover, BMP is critical for the progression of neuropathic pain by activating astrocytes through the downstream *p*-Smad1/5/8 signaling pathway. In line with these findings, we discovered that Smad1 is also required for the BMP2-induced upregulation of CGRP expression in our rat model of BCP. Therefore, we propose that once BMP2 binds to BMPRs, it phosphorylates downstream Smad1 and triggers the Smad signaling pathway to affect the expression of CGRP, which in turn sensitizes sensory neurons and causes BCP in rats.

However, there are several limitations for this study. Firstly, there is evidence that CGRP effects are sex dependent [52], while we mainly focused on the important role of BMP2-Smad1-CGRP signaling pathway in the progression of BCP, so that was why we only

chose female rats in this study. The roles of BMP2 and CGRP in the progression of BCP in other gender or species require further investigation. Secondly, other cancers like lung cancer, prostate cancer tend to metastasize to bone and cause insufferable pain [2], and whether the same observation in this study can be observed in other metastatic bone cancers need further investigation. Moreover, in this study, we only detected upregulation of BMP2 in DRG neurons. However, due to the multi-biofunction of BMP2, whether expression change of BMP2 from other tissues or cells such as bone microenvironment [53] or cancer cells [54] contribute to BCP still need further investigation. Last but not least, there are evidences indicating that multiple factors such as increased fibrinogen, melatonin, or activated Wnt signaling could activate BMP signaling [55–57], while in the progression of BCP, the upstream molecules which cause the increased expression of BMP2 in the DRG are still unclear and need further investigation. Despite the limitations, we demonstrated that BMP2 can upregulate CGRP expression in DRG neurons by activating the BMPR/Smad1 signaling pathway, therefore induce BCP. Targeting BMP2-Smad1-CGRP signaling pathway may become a novel potential therapeutic strategy for BCP treatment.

5. Conclusion

The current study reveals that the activation of BMP2/Smad1 signaling leads to BCP in rats by upregulating CGRP expression in sensory neurons of the DRG. These findings might offer a novel approach to the investigation and treatment of BCP.

Ethics statement

The study protocol was approved by the Animal Care and Use Committee of Shanghai Chest Hospital, Shanghai Jiao Tong University, School of Medicine [permission no. KS (Y)20186].

Fundings

This study was supported by the National Natural Science Foundation of China (No. 82071233 to **JW**) and Shanghai Sailing Program (No. 21YF1442900 to **WW**).

Data availability statement

The data are available from the corresponding author on reasonable request.

CRediT authorship contribution statement

Wei Wang: Writing – original draft, Methodology, Investigation, Funding acquisition, Data curation, Conceptualization. **Zhihao Gong:** Writing – original draft, Methodology, Investigation, Data curation, Conceptualization. **Kai Wang:** Investigation. **Mi Tian:** Investigation. **Yuxin Zhang:** Investigation, Data curation. **Xin Li:** Investigation, Data curation. **Xingji You:** Writing – review & editing, Supervision, Methodology, Conceptualization. **Jingxiang Wu:** Writing – review & editing, Supervision, Methodology, Funding acquisition, Conceptualization.

Declaration of competing interest

The authors declare that they have no known competing financial interests or personal relationships that could have appeared to influence the work reported in this paper.

Appendix A. Supplementary data

Supplementary data to this article can be found online at doi:mmcdoino

References

[1] F. Bray, A. Jemal, N. Grey, J. Ferlay, D. Forman, Global cancer transitions according to the Human Development Index (2008-2030): a population-based study, Lancet Oncol. 13 (8) (2012) 790–801.
[2] K.N. Weilbaecher, T.A. Guise, L.K. McCauley, Cancer to bone: a fatal attraction, Nat. Rev. Cancer 11 (6) (2011) 411–425.
[3] K. Wang, Y. Gu, Y. Liao, S. Bang, C.R. Donnelly, O. Chen, X. Tao, A.J. Mirando, M.J. Hilton, R.R. Ji, PD-1 blockade inhibits osteoclast formation and murine bone cancer pain, J. Clin. Invest. 130 (7) (2020) 3603–3620.
[4] X.T. He, X.F. Hu, C. Zhu, K.X. Zhou, W.J. Zhao, C. Zhang, X. Han, C.L. Wu, Y.Y. Wei, W. Wang, J.P. Deng, F.M. Chen, Z.X. Gu, Y.L. Dong, Suppression of histone deacetylases by SAHA relieves bone cancer pain in rats via inhibiting activation of glial cells in spinal dorsal horn and dorsal root ganglia, J. Neuroinflammation 17 (1) (2020) 125.
[5] P. Mantyh, Bone cancer pain: causes, consequences, and therapeutic opportunities, Pain 154 (Suppl 1) (2013) S54–s62.
[6] L. Ye, M.D. Mason, W.G. Jiang, Bone morphogenetic protein and bone metastasis, implication and therapeutic potential, Front. Biosci. 16 (3) (2011) 865–897.
[7] S. Kishigami, Y. Mishina, BMP signaling and early embryonic patterning, Cytokine Growth Factor Rev. 16 (3) (2005) 265–278.

[8] M.J. Goumans, A. Zwijsen, P. Ten Dijke, S. Bailly, Bone morphogenetic proteins in vascular homeostasis and disease, Cold Spring Harbor Perspect. Biol. 10 (2) (2018).
[9] A.B. Core, S. Canali, J.L. Babitt, Hemojuvelin and bone morphogenetic protein (BMP) signaling in iron homeostasis, Front. Pharmacol. 5 (2014) 104.
[10] L. Grgurevic, G.L. Christensen, T.J. Schulz, S. Vukicevic, Bone morphogenetic proteins in inflammation, glucose homeostasis and adipose tissue energy metabolism, Cytokine Growth Factor Rev. 27 (2016) 105–118.
[11] D.H. Wu, A.K. Hatzopoulos, Bone morphogenetic protein signaling in inflammation, Exp. Biol. Med. (Maywood, NJ, U. S.) 244 (2) (2019) 147–156.
[12] B. Gámez, E. Rodriguez-Carballo, F. Ventura, BMP signaling in telencephalic neural cell specification and maturation, Front. Cell. Neurosci. 7 (2013) 87.
[13] J. Shen, A.W. James, J.N. Zara, G. Asatrian, K. Khadarian, J.B. Zhang, S. Ho, H.J. Kim, K. Ting, C. Soo, BMP2-induced inflammation can be suppressed by the osteoinductive growth factor NELL-1, Tissue Eng Part A 19 (21–22) (2013) 2390–2401.
[14] E. Carlisle, J.S. Fischgrund, Bone morphogenetic proteins for spinal fusion, Spine J. 5 (6 Suppl) (2005) 240s–249s.
[15] K. Mitchell, J.P. Shah, C.L. Dalgard, L.V. Tsytsikova, A.C. Tipton, A.E. Dmitriev, A.J. Symes, Bone morphogenetic protein-2-mediated pain and inflammation in a rat model of posterolateral arthrodesis, BMC Neurosci. 17 (1) (2016) 80.
[16] J.N. Zara, R.K. Siu, X. Zhang, J. Shen, R. Ngo, M. Lee, W. Li, M. Chiang, J. Chung, J. Kwak, B.M. Wu, K. Ting, C. Soo, High doses of bone morphogenetic protein 2 induce structurally abnormal bone and inflammation in vivo, Tissue Eng Part A 17 (9–10) (2011) 1389–1399.
[17] L.B. Shields, G.H. Raque, S.D. Glassman, M. Campbell, T. Vitaz, J. Harpring, C.B. Shields, Adverse effects associated with high-dose recombinant human bone morphogenetic protein-2 use in anterior cervical spine fusion, Spine 31 (5) (2006) 542–547.
[18] L. Yang, S. Liu, Y. Wang, Role of bone morphogenetic protein-2/4 in astrocyte activation in neuropathic pain, Mol. Pain 15 (2019) 1744806919892100.
[19] V. Nguyen, C.A. Meyers, N. Yan, S. Agarwal, B. Levi, A.W. James, BMP-2-induced bone formation and neural inflammation, J. Orthop. 14 (2) (2017) 252–256.
[20] H. Tian, C.S. Li, T.P. Scott, S.R. Montgomery, K. Phan, L. Lao, W. Zhang, Y. Li, T. Hayashi, S. Takahashi, R. Alobaidaan, M. Ruangchainikom, K.W. Zhao, E. J. Brochmann, S.S. Murray, J.C. Wang, M.D. Daubs, Secreted phosphoprotein 24 kD inhibits nerve root inflammation induced by bone morphogenetic protein-2, Spine J. 15 (2) (2015) 314–321.
[21] A.E. Dmitriev, S. Farhang, R.A. Lehman Jr., G.S. Ling, A.J. Symes, Bone morphogenetic protein-2 used in spinal fusion with spinal cord injury penetrates intrathecally and elicits a functional signaling cascade, Spine J. 10 (1) (2010) 16–25.
[22] A.E. Dmitriev, R.A. Lehman Jr., A.J. Symes, Bone morphogenetic protein-2 and spinal arthrodesis: the basic science perspective on protein interaction with the nervous system, Spine J. 11 (6) (2011) 500–505.
[23] R.C. Bucelli, E.A. Gonsiorek, W.Y. Kim, D. Bruun, R.A. Rabin, D. Higgins, P.J. Lein, Statins decrease expression of the proinflammatory neuropeptides calcitonin gene-related peptide and substance P in sensory neurons, J. Pharmacol. Exp. Therapeut. 324 (3) (2008) 1172–1180.
[24] F.A. Russell, R. King, S.J. Smillie, X. Kodji, S.D. Brain, Calcitonin gene-related peptide: physiology and pathophysiology, Physiol. Rev. 94 (4) (2014) 1099–1142.
[25] A. Charles, P. Pozo-Rosich, Targeting calcitonin gene-related peptide: a new era in migraine therapy, Lancet 394 (10210) (2019) 1765–1774.
[26] L. Edvinsson, K.A. Haanes, K. Warfvinge, D.N. Krause, CGRP as the target of new migraine therapies - successful translation from bench to clinic, Nat. Rev. Neurol. 14 (6) (2018) 338–350.
[27] X. Ai, J. Cappuzzello, A.K. Hall, Activin and bone morphogenetic proteins induce calcitonin gene-related peptide in embryonic sensory neurons in vitro, Mol. Cell. Neurosci. 14 (6) (1999) 506–518.
[28] W. Wang, Q. Jiang, J. Wu, W. Tang, M. Xu, Upregulation of bone morphogenetic protein 2 (Bmp2) in dorsal root ganglion in a rat model of bone cancer pain, Mol. Pain 15 (2019) 1744806918824250.
[29] A.D. Bennett, K.M. Chastain, C.E. Hulsebosch, Alleviation of mechanical and thermal allodynia by CGRP(8-37) in a rodent model of chronic central pain, Pain 86 (1–2) (2000) 163–175.
[30] R.R. Hansen, V. Vacca, T. Pitcher, A.K. Clark, M. Malcangio, Role of extracellular calcitonin gene-related peptide in spinal cord mechanisms of cancer-induced bone pain, Pain 157 (3) (2016) 666–676.
[31] S.N. Raja, D.B. Carr, M. Cohen, N.B. Finnerup, H. Flor, S. Gibson, F.J. Keefe, J.S. Mogil, M. Ringkamp, K.A. Sluka, X.J. Song, B. Stevens, M.D. Sullivan, P. R. Tutelman, T. Ushida, K. Vader, The revised International Association for the Study of Pain definition of pain: concepts, challenges, and compromises, Pain 161 (9) (2020) 1976–1982.
[32] S.J. Medhurst, K. Walker, M. Bowes, B.L. Kidd, M. Glatt, M. Muller, M. Hattenberger, J. Vaxelaire, T. O'Reilly, G. Wotherspoon, J. Winter, J. Green, L. Urban, A rat model of bone cancer pain, Pain 96 (1–2) (2002) 129–140.
[33] B. Remeniuk, D. Sukhtankar, A. Okun, E. Navratilova, J.Y. Xie, T. King, F. Porreca, Behavioral and neurochemical analysis of ongoing bone cancer pain in rats, Pain 156 (10) (2015) 1864–1873.
[34] N.M. Luger, D.B. Mach, M.A. Sevcik, P.W. Mantyh, Bone cancer pain: from model to mechanism to therapy, J. Pain Symptom Manag. 29 (5 Suppl) (2005) S32–S46.
[35] A. Nohe, S. Hassel, M. Ehrlich, F. Neubauer, W. Sebald, Y.I. Henis, P. Knaus, The mode of bone morphogenetic protein (BMP) receptor oligomerization determines different BMP-2 signaling pathways, J. Biol. Chem. 277 (7) (2002) 5330–5338.
[36] T.L. Follansbee, K.J. Gjelsvik, C.L. Brann, A.L. McParland, C.A. Longhurst, M.J. Galko, G.K. Ganter, Drosophila nociceptive sensitization requires BMP signaling via the canonical SMAD pathway, J. Neurosci. 37 (35) (2017) 8524–8533.
[37] C.A. Tannoury, H.S. An, Complications with the use of bone morphogenetic protein 2 (BMP-2) in spine surgery, Spine J. 14 (3) (2014) 552–559.
[38] M.G. Lykissas, A. Aichmair, A.P. Hughes, A.A. Sama, D.R. Lebl, F. Taher, J.Y. Du, F.P. Cammisa, F.P. Girardi, Nerve injury after lateral lumbar interbody fusion: a review of 919 treated levels with identification of risk factors, Spine J. 14 (5) (2014) 749–758.
[39] P. Huang, A. Chen, W. He, Z. Li, G. Zhang, Z. Liu, G. Liu, X. Liu, S. He, G. Xiao, F. Huang, J. Stenvang, N. Brünner, A. Hong, J. Wang, BMP-2 induces EMT and breast cancer stemness through Rb and CD44, Cell Death Dis. 3 (2017) 17039.
[40] D. Halloran, H.W. Durbano, A. Nohe, Bone morphogenetic protein-2 in development and bone homeostasis, J. Dev. Biol. 8 (3) (2020).
[41] J.A. Rihn, R. Patel, J. Makda, J. Hong, D.G. Anderson, A.R. Vaccaro, A.S. Hilibrand, T.J. Albert, Complications associated with single-level transforaminal lumbar interbody fusion, Spine J. 9 (8) (2009) 623–629.
[42] E.A. Meyers, J.A. Kessler, TGF-B family signaling in neural and neuronal differentiation, development, and function, Cold Spring Harbor Perspect. Biol. 9 (8) (2017).
[43] I.L. Gibbins, J.B. Furness, M. Costa, Pathway-specific patterns of the co-existence of substance P, calcitonin gene-related peptide, cholecystokinin and dynorphin in neurons of the dorsal root ganglia of the Guinea-pig, Cell Tissue Res. 248 (2) (1987) 417–437.
[44] M. Southwood, T.K. Jeffery, X. Yang, P.D. Upton, S.M. Hall, C. Atkinson, S.G. Haworth, S. Stewart, P.N. Reynolds, L. Long, R.C. Trembath, N.W. Morrell, Regulation of bone morphogenetic protein signalling in human pulmonary vascular development, J. Pathol. 214 (1) (2008) 85–95.
[45] L. Zhang, A.O. Hoff, S.J. Wimalawansa, G.J. Cote, R.F. Gagel, K.N. Westlund, Arthritic calcitonin/alpha calcitonin gene-related peptide knockout mice have reduced nociceptive hypersensitivity, Pain 89 (2–3) (2001) 265–273.
[46] B.A. Cruise, P. Xu, A.K. Hall, Wounds increase activin in skin and a vasoactive neuropeptide in sensory ganglia, Dev. Biol. 271 (1) (2004) 1–10.
[47] P. Xu, A.K. Hall, The role of activin in neuropeptide induction and pain sensation, Dev. Biol. 299 (2) (2006) 303–309.
[48] M.C. Gomez-Puerto, P.V. Iyengar, A. García de Vinuesa, P. Ten Dijke, G. Sanchez-Duffhues, Bone morphogenetic protein receptor signal transduction in human disease, J. Pathol. 247 (1) (2019) 9–20.
[49] Y.E. Zhang, Non-Smad pathways in TGF-beta signaling, Cell Res. 19 (1) (2009) 128–139.
[50] K. Yamaguchi, K. Shirakabe, H. Shibuya, K. Irie, I. Oishi, N. Ueno, T. Taniguchi, E. Nishida, K. Matsumoto, Identification of a member of the MAPKKK family as a potential mediator of TGF-beta signal transduction, Science 270 (5244) (1995) 2008–2011.
[51] R. Derynck, Y.E. Zhang, Smad-dependent and Smad-independent pathways in TGF-beta family signalling, Nature 425 (6958) (2003) 577–584.
[52] B.J. Rea, A. Davison, M.J. Ketcha, K.J. Smith, A.M. Fairbanks, A.S. Wattiez, P. Poolman, R.H. Kardon, A.F. Russo, L.P. Sowers, Automated detection of squint as a sensitive assay of sex-dependent calcitonin gene-related peptide and amylin-induced pain in mice, Pain 163 (8) (2022) 1511–1519.

[53] X. Wu, S.M. Chim, V. Kuek, B.S. Lim, S.T. Chow, J. Zhao, S. Yang, V. Rosen, J. Tickner, J. Xu, HtrA1 is upregulated during RANKL-induced osteoclastogenesis, and negatively regulates osteoblast differentiation and BMP2-induced Smad1/5/8, ERK and p38 phosphorylation, FEBS Lett. 588 (1) (2014) 143–150.
[54] F. Huang, Y. Cao, G. Wu, J. Chen, C. Wang, W. Lin, R. Lan, B. Wu, X. Xie, J. Hong, L. Fu, BMP2 signalling activation enhances bone metastases of non-small cell lung cancer, J. Cell Mol. Med. 24 (18) (2020) 10768–10784.
[55] M.A. Petersen, J.K. Ryu, K.J. Chang, A. Etxeberria, S. Bardehle, A.S. Mendiola, W. Kamau-Devers, S.P.J. Fancy, A. Thor, E.A. Bushong, B. Baeza-Raja, C.A. Syme, M.D. Wu, P.E. Rios Coronado, A. Meyer-Franke, S. Yahn, L. Pous, J.K. Lee, C. Schachtrup, H. Lassmann, E.J. Huang, M.H. Han, M. Absinta, D.S. Reich, M. H. Ellisman, D.H. Rowitch, J.R. Chan, K. Akassoglou, Fibrinogen activates BMP signaling in Oligodendrocyte progenitor cells and inhibits remyelination after vascular damage, Neuron 96 (5) (2017) 1003–1012.e7.
[56] R. Zhao, L. Tao, S. Qiu, L. Shen, Y. Tian, Z. Gong, Z.B. Tao, Y. Zhu, Melatonin rescues glucocorticoid-induced inhibition of osteoblast differentiation in MC3T3-E1 cells via the PI3K/AKT and BMP/Smad signalling pathways, Life Sci. 257 (2020) 118044.
[57] M.C. Verhoeven, C. Haase, V.M. Christoffels, G. Weidinger, J. Bakkers, Wnt signaling regulates atrioventricular canal formation upstream of BMP and Tbx2, Birth Defects Res A Clin Mol Teratol 91 (6) (2011) 435–440.